

Mechanised TIG Welding Gives Consistent Bead Geometry, A Case Study

Akhilesh Kumar Singh, Vidyut Dey, Ram Naresh Rai

Department of Production Engineering
National Institute of Technology, Agartala
Tripura(w) - 799046, India
akhileshkr.singh@hotmail.com
Mb.: +91-9416458278

Abstract:- In the present study, TIG (Tungsten Inert Gas) bead-on-plate welding is carried out on grade P91 steel plates of size 100 mm x 50 mm x 6 mm. Grade P91 steel, is basically a Creep Strength-Enhanced Ferritic Steel (CSEF) known as the modified 9Cr-1Mo-V and is designated as P91 steel for Plate (A 387/A387M). The experiment is conducted with pure argon gas, without any filler material. Three control parameters (current, travel speed and gas flow rate) are taken in to consideration for autogenous fusion arc welding. In TIG welding, when the movement of either the torch or the workpiece is manually controlled, the electrode gap and the travel speed is difficult to control. The quality of the weld bead characteristics, thus, is affected. A setup with a motor-controlled travel-speed machine has been fabricated to avoid human errors during welding. The responses, weld bead geometry (in terms of bead width, depth of penetration), weld area, and width of Heat Affected Zone (HAZ) width have been measured and compared for both manual as well as mechanized welding. It has been found that the bead geometric parameters are more consistent when welded with the mechanized setup compared to manual welding.

Keywords: TIG welding, CSEF, Weld Bead Geometry, control parameters

1. INTRODUCTION

Modified 9Cr-1Mo-V (P91) steel is widely used in different high temperature components of power- generating applications and also receiving the greatest attention from researchers and fabricators worldwide today[1]. Modified 9Cr-1Mo-V, designated as Grade 91 (for Plate) - A 387/A387M, Grade P91 steel, basically is a Creep Strength – Enhanced Ferritic Steel (CSEF) known as the its Standard Specification for Pressure Vessel Plates, Alloy Steel, Chromium – Molybdenum[2]. In different power industries the modified 9Cr-1Mo-V steel plates used in the form of steam header, steam pipes, superheater, pressure vessel plates, reheater and in process vessels of chemical industries[3]. Grade P91 have other desirable properties than other modified XCr-Mo-V steel such as stress corrosion cracking (SCC) resistance, low thermal expansion, high thermal conductivity, good resistance to thermal fatigue, excellent creep resistance and also good weldability [4-8]. The modified 9Cr-1Mo-V steel plates extremely hardenable

material are used at a higher steam temperature more than 600°C and a steam pressure greater than 35 MPa[9].

A case study has been carried out to analyse the bead geometry characteristics. The Bead-on-plate welding is performed on 6 mm thick plates. The plates are welded by two methods: one by hand held moving torch and the other by fixed torch with the work pieces moved by a motor-controlled trolley. The micro structures and the micro-hardness of the plates welded by the above two methods are compared.

2. EXPERIMENTS

Tungsten inert gas (TIG) welding process is generally used to produce high quality weld joints of 9Cr-1Mo steel[10]. Bead on plate welding experiment was performed on Grade P-91 steel plates on 6 mm thick plate by tungsten inert gas (TIG) technique to investigate the effect of both the methods - manually and motor-controlled travel-speed to analyse the bead geometry structures. The chemical composition of Grade P-91 steel plate's material is shown in Table 1.

Table 1: The chemical composition of material used

	Cr %	Mo %	V %	N2 %	C %	Si %	Mn %	P %	S %	Ni %	Al %
P91 Steel Plate (6 mm Thickness)	8.81	0.97	0.24	0.046	0.093	0.32	0.44	0.018	0.007	0.15	0.015

Experiment is carried out on three input process parameters (i.e. current, travel speed and gas flow rate) is shown in Table 2. For welding, the specimen P91 steel plate material was cut into size of 100mm x 50mm x 6mm by abrasive cutter with blade of thickness 1.5 mm was used to cut the specimens at 1500 rpm. Two types of welding have been performed: First - Workpiece fixed and torch travel-speed handle – manually. Second - Workpiece fixed and torch travel-speed controlled by travel-speed machine has been fabricated to avoid human errors during welding.

After welding, the specimens were cut by abrasive cutter then grinded, polished and etched, using 5% Nital, to reveal the bead geometry on the cross section. The etched specimens were then photographed using a digital camera, shown in Fig. 1 and 2 which were later used for dimension measurement.

Table 2: The Input Process Parameters

Sample No.	Welding Current (A) C	Gas flow rate (l/min) G	Motor-controlled travel-speed Welding Time (cm/min) Sa	Manually-controlled travel-speed Welding Time (cm/min) Sm
a	150	8	15	14
b	200	10	17.5	21
c	250	12	25	22

3. RESULTS AND DISCUSSION

To recognise the weld bead geometry, the welded specimens were cut by abrasive cutter then grinded, polished and etched to reveal the bead geometry on the cross section. Photographed taken from a digital camera. To recognize the digital camera pixel intensity and image capture distance of specimens, we pasted the (1 cm) scale on the specimen to measure accurate dimension. The responses, dimensions measurement of weld bead geometry (in terms of bead width, depth of penetration), weld area, and width of Heat Affected Zone (HAZ) have been measured with the help of Adobe Acrobat 9.0 Pro software. Measured data is shown in Table 3 and 4.

3.1 Motor-Controlled and Manually-Controlled Travel-Speed Welding

Fig.1 (a-c) show welds bead geometry welded by motor operated trolley. Fig.1 (b) shows the weld bead geometry in which the crown of the weld bead is very prominent even though the welding is autogenous. Fig.2 (a-c) show the weld bead geometry when the torch was manually moved. It can be clearly seen from the photographs that the area of the heat affected zones are more when the torch was moved manually over the plates. On the other hand penetration of the welds is more when the plates were welded with a motor controlled trolley. An interesting feature is seen in Fig 1c and 2c. In both the cases the penetration has taken a ‘W’ shape. The reason for such shape needs to be investigated in future.



Fig.1- Etched cross-section of motor-controlled travel-speed welding showing bead geometry



Fig.2- Etched cross-section of manually-controlled travel-speed welding showing bead geometry

Table 3: Bead geometry of welds done by motor controlled trolley

Sample Number	Measured Data of Motor-Controlled Travel-Speed Welding			
	Width (cm)	Penetration (cm)	Area (cm ²)	Width HAZ (cm)
a	0.438	0.328	0.116	0.129
b	0.624	0.252	0.111	0.129
c	0.816	0.287	0.174	0.146

Table 4: Bead geometry of welds done by hand-controlled welding torch

Sample Number	Measured Data of Manually-Controlled Travel-Speed Welding			
	Width (cm)	Penetration (cm)	Area (cm ²)	Width HAZ (cm)
a	0.929	0.125	0.081	0.134
b	0.672	0.233	0.112	0.188
c	0.883	0.234	0.147	0.111

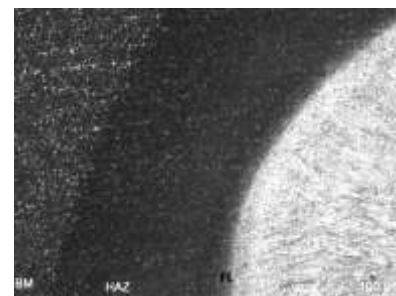
3.2 Microstructures after TIG Welding

The microstructures of weld bead geometry and Heat Affected Zone (HAZ) have been analysis by optical microscope (Lieca Qwin software). The microstructures of motor-controlled and manually controlled travel-speed welding are shown in the Figures. (3-4). Autogenous fusion gas (TIG) welding, bead-on-plate weld is carried out on grade P91 steel plates of size 6 mm thick specimen are used. The microstructures of all the welds show equiaxed grains with varying shape and size.

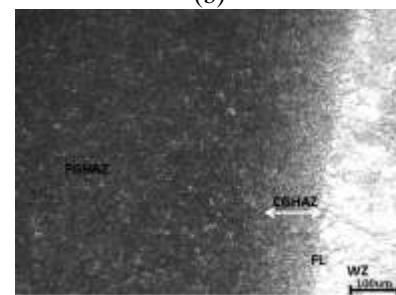
It has been seen that the HAZ areas consists of different sub-zones with varying microstructure as shown in Fig. (3-4). The specific microstructure depends on the related thermal profile generated by a particular welding condition [11].



(a)



(b)



(c)

Fig.3- The microstructures of specimen welded by motor-controlled travel-speed welding: (a) C1Sa1G1, (b) C2Sa2G2 and (c) C3Sa3G3

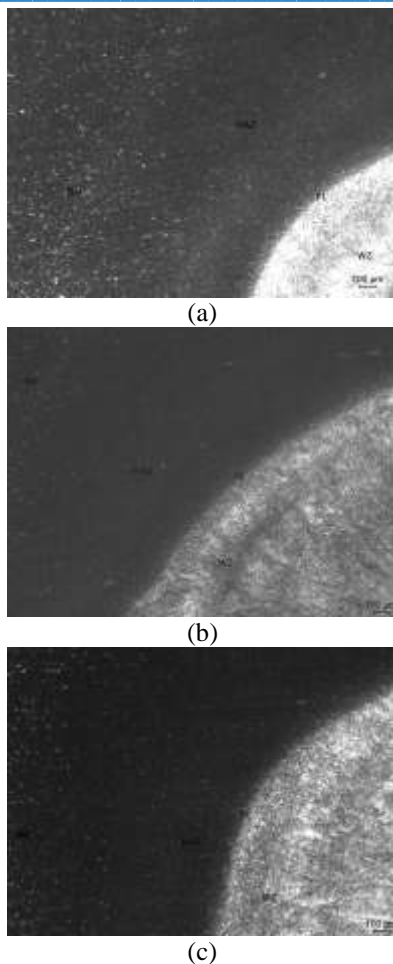


Fig.4- - The microstructures of specimen welded by hand-controlled torch:
 (a) C1Sm1G1, (b) C2Sm2G2 and (c) C3Sm3G3

After performing the basic operation of welding image measurement and microstructure the specimen is further used for micro-hardness to analysis the mechanical properties of welding parameter and process used.

3.3 Hardening Behaviour

Hardness is the property of a material to resist the plastic deformation. For hardness measurement - specimen P91 steel plate material was cut into size of 50mm x 5mm x 6mm by abrasive cutter with blade then grinded, polished and etched, using 5% Nital, to reveal the bead geometry on the cross section.

Hardness testing was carried out in a straight line 2 mm below and parallel to surface of the base plate with a constant load of 1 Kg and dwell time 10 sec. Reading were taken 0.5 steps through the WZ, HAZ and the part of the base material. Hardness testing was carried out according to ASTM designation: E384 – 11, Standard Test Method for Knoop and Vickers Hardness of Materials [12].

Fig. 5(a) shows hardness profiles across the entire motor-controlled travel-speed machine weld. Hardness of the weld metal is more uniform across the weld bead geometries region to heat affected zone (HAZ). The HAZ can be further divided into Coarse grained heat affected zone (CGHAZ) and Fine grained heat affected zone (FGHAZ). Hardness is higher at CGHAZ region in second specimens i.e. C2Sa2M2 of the welds region and hardness decrease toward the base metal. Fig. 5(b) shows hardness profiles across the entire manual-controlled travel-speed machine weld. Hardness is higher at weld zone (WZ) region in all specimens and hardness decrease toward the base metal.

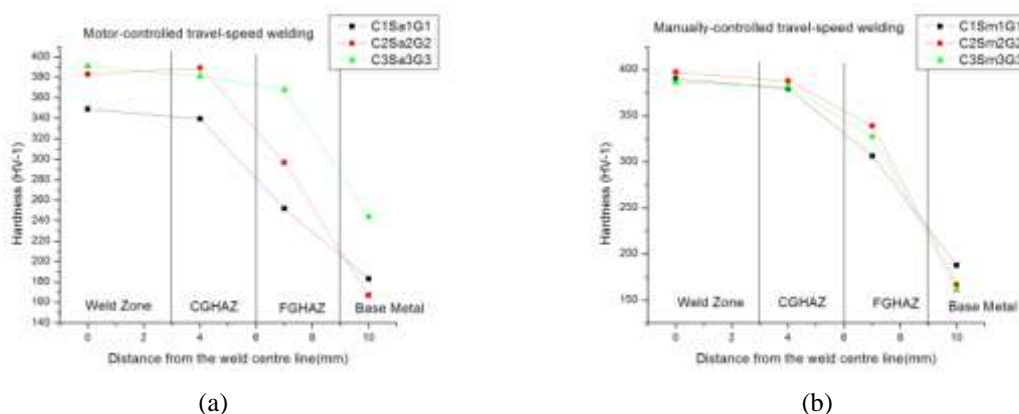


Fig.5- (a) Show the Motor-controlled travel-speed welding and (b) Manually-controlled travel-speed welding

4. CONCLUSION

In this study, the weld bead geometry is studied with respect to the way the torch is handled i.e. whether the torch remains fixed or is moved manually. It has been found that the bead geometry is more consistent when welded with the mechanized setup compared to manual welding. The effect of variation in welding parameters on hardness of the weld is pronouncedly visible when welding is done with torch

fixed and a mechanised trolley. In both autogenous TIG welding process mentioned above, hardness is higher at weld zone (WZ) and thereafter decrease toward the base metal. In only one specimen we observed higher hardness at CGHAZ region in C2Sa2M2. The reason of such variation has to be investigated in a future study of the welds region and then hardness decrease toward the base metal.

5. REFERENCES

- [1] Arivazhagan, B., Sundaresan, S., and Kamaraj, M., "A study on influence of shielding gas composition on toughness of flux-cored arc weld of modified 9Cr-1Mo (P91) steel" *Journal of Materials Processing Technology*, Volume 209, Issues 12–13, Pages 5245–5253, 1 July 2009.
- [2] ASTM, Designation: A387/A387M-06a, "Standard Specification for Pressure Vessel Plates, Alloy Steel, Chromium-Molybdenum".
- [3] Hasegawa, Y., Ohgami, M., Okamura, Y., Viswanathan, R., and Nutting (Eds.), J., "Advanced Heat Resistant Steel for Power Generation", The University Press, Cambridge, Pages. 655–667, UK (1999).
- [4] Arivazhagan, B., and Kamaraj, M., "Metal-cored arc welding process for joining of modified 9Cr-1Mo (P91) steel", *Journal of Manufacturing Processes*, Volume 15, Issue 4, Pages 542–548, October 2013.
- [5] Onoro, J., "Martensite microstructure of 9-12% Cr steels weld metals", *Journal of Materials Processing Technology* (2006), Pages 137–142.
- [6] Sikka, V., Ward, C.T., Thomas, K.C., and Khare (Ed.), A.K., "Modified 9Cr-1Mo Steel—An Improved Alloy for Steam Generator Application in Ferritic Steels for High-Temperature Applications", American Society for Metals, Metals Park, OH, Pages 65–84 (1983).
- [7] Brozda, J., Lomozik, M., and Zeman, M., "A welding of P91 steel to other grades of steel for elevated temperature service", *Welding International* 12(7), Pages 509-518. 1998.
- [8] Gianfrancesco, A. Di., Tassa, O., Matera, S., Cumino, G., Viswanathan, R., Nutting (Eds.), J., "Advanced Heat Resistant Steel for Power Generation", The University Press, Cambridge, UK, Pages 622–632 (1999). [9] Milovic, L., Manjgo, M., Andelic, N., Milosevic, V., Je;I, Z., and Dondur, N., "Behaviour of P91 steel simulated HAZ at 600°C", 15th International Research/Expert Conference "Trends in the Development of Machinery and Associated Technology" TMT 2011, Prague, Czech Republic, September 2011, Pages 12-18.
- [10] Arunkumar, V., Vasudevan, M., Maduraimuthu, V., and Muthupandi, V., "Effect of Activated Flux on the Microstructure and Mechanical Properties of 9Cr-1Mo Steel Weld Joint" *Materials and Manufacturing Processes*, Volume 27, Issue 11, pages 1171-1177, 2012.
- [11] Kapustka, N., Conrardy, C., Babu, S., and Albright, C., "Effect of GMAW Process and Material Conditions on DP 780 and TRIP 780 Welds", Supplement to the *Welding Journal*, *Welding Research*, Vol. 87, pages 135-148, June 2008.
- [12] ASTM, Designation: E384 – 11, Standard Test Method for Knoop and Vickers Hardness of Materials.